Chemical Papers (2023) 77:2295–2308
https://doi.org/10.1007/s11696-022-02629-8

ORIGINAL PAPER

Dye-encapsulated metal–organic framework composites for highly sensitive and selective sensing of oxytetracycline based on ratiometric fluorescence

Peng-Chen Su[1,2,3] · Long Yu[1,2] · Mi Yuan[2,4] · Ling-Xiao Wang[1,2] · Ming-Tai Sun[2] · Wei-Jie Hu[2] · Hua Tan[2] · Su-Hua Wang[1,2]

Received: 3 October 2022 / Accepted: 10 December 2022 / Published online: 21 December 2022

Abstract

Herein, we reported a class of well-fluorescence-stabilized rare-earth-free ratiometric fluorescent probe for highly sensitive visual detection of oxytetracycline (OTC), which was fabricated by encapsulation of blue-emitting dye 2-aminoterephthalic acid into nanopores of aluminum-based metal–organic framework MIL-53(Al) with microflower morphology (denoted as FMIL-53(Al)). The surface-distributed abundant open aluminum sites of FMIL-53(Al) can coordinate and fix the conformation of OTC molecules, which selectively increases the fluorescent quantum yield of OTC at ~ 520 nm. The dye in the probe is inert to the analyte, and the blue fluorescence intensity is constant. When the green fluorescence of OTC increases, a continuous color evolution from blue to green is observed. For sensing applications, NH_2-BDC@FMIL-53(Al)-3 was selected as the sensor. The optimized conditions for the sensing process were as follows: sensing medium was HEPES buffer (10 mM, pH = 7.3), probe concentration: 0.1 mg/mL; incubation time: 45 min; optimal excitation wavelength: 383 nm. The detection limit was estimated to be 11.0 nM, which is considered to be one of the most sensitive ratiometric fluorescent probes for OTC detection. More importantly, a smartphone-based sensing method was developed, providing a promising non-instrument-based technique for the reliable, semi-quantitative assay of OTC in the field.

✉ Su-Hua Wang
wangsuhua@ncepu.edu.cn

[1] MOE Key Laboratory of Resources and Environmental System Optimization, College of Environmental Science and Engineering, North China Electric Power University, Beijing 102206, People's Republic of China

[2] School of Environmental Science and Engineering, Guangdong University of Petrochemical Technology, Maoming 525000, People's Republic of China

[3] Department of Chemical Engineering, Hebei Petroleum University of Technology, Chengde 067000, People's Republic of China

[4] College of Biomedicine and Health, Huazhong Agricultural University, Wuhan 430070, People's Republic of China

Graphical abstract

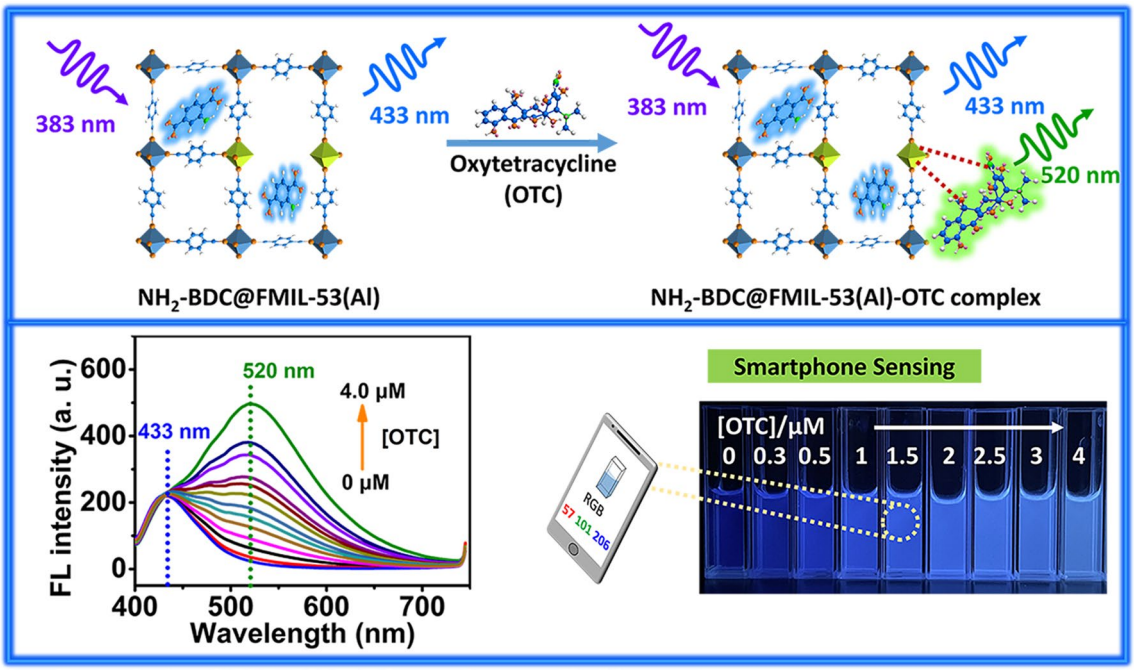

Keywords Ratiometric fluorescence · Oxytetracycline (OTC) · Visual monitoring · Smartphone platform

Introduction

Oxytetracycline (OTC), as an inexpensive broad-spectrum antibiotic, has been used extensively worldwide as a feed additive in livestock and poultry or fish farming for preventive control or therapy of bacterial infections (Anadón et al. 2016; Simon 2005). However, the abuse of OTC leads to its excessive residue in animal-derived foods, which poses many threats to humans, including allergic reactions, liver/kidney toxicity, gastrointestinal problems, etc. (Anadón et al. 2016). More alarming, environmental residual OTC can induce the generation of antibiotic resistance genes, leading to the evolution of antibiotic-resistant bacteria, which might seriously damage the micro-ecological balance and thus, threaten human health (Anadón et al. 2016; Simon 2005). Therefore, it is much-needed to establish reliable analytical methods to quantify OTC accurately.

To date, various types of instrument-based OTC analysis methods have been suggested, namely high-performance liquid chromatography-tandem mass spectrometry (HPLC-TMS) (Gajda 2017), enzyme-linked immunosorbent assay (ELISA) (Chen et al. 2016), immunochromatographic assay (ICA) (Sheng et al. 2018), surface-enhanced Raman scattering (SERS) (Meng et al. 2017) and so on. Being very informative, these instrument-based methods require expensive apparatus and specialized technicians (Wang et al. 2018). In this framework, fluorescence-based assays provide a powerful method for the simple and efficient detection of trace amounts of OTC (Esmaelpourfarkhani et al. 2019; Kuong et al. 2009; Li et al. 2019, 2020a, b; Sun et al. 2022; Wang et al. 2005). However, most of the currently reported probes for OTC sensing are single-color fluorescence-based sensors, including "turn-off" (Li et al. 2019, 2020a, b) or "turn-on" (Esmaelpourfarkhani et al. 2019; Kuong et al. 2009; Wang et al. 2005) sensors. By contrast, ratiometric methods based on dual-color fluorescence signals provide a built-in correction against external interferences (Qian et al. 2020; Xu et al. 2022; Yuan et al. 2023; Zhang et al. 2022), and the relative change in intensities of the two peaks caused by the addition of an analyte can be externalized as a consecutive color change recognizable to the naked eye, allowing rapid visual identification (Qian et al. 2020; Xu et al. 2022; Yuan et al. 2023). However, fluorescent probes for ratiometric detection of OTC were reported rarely, and most of them are rare-earth elements containing probes that involve the "antenna effect" mechanism (Chen et al. 2020a; Sun et al. 2022; Yang et al. 2021). Unfortunately, the use of rare-earth elements in fluorescent probes not only implies higher costs, but also potential supply deficiencies, and severe adverse environmental impacts. Therefore, it is crucial to design reliable ratiometric fluorescent probes,

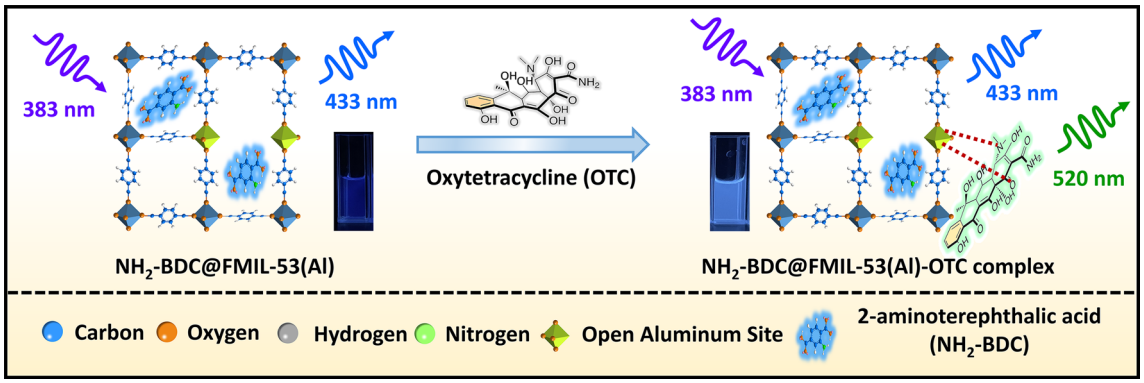

Scheme 1 Schematic illustration of OTC detection based on the constructed ratiometric fluorescent probe NH_2-BDC@FMIL-53(Al)

especially rare-earth-free ratiometric fluorescent probes, for sensitive and rapid detection of OTC.

Metal–organic frameworks are a class of porous hybrid crystalline materials formed during the self-assembly of metal nodes and organic ligands (Zhao et al. 2021; Su et al. 2022a). Characterized by inexpensive and readily available raw materials, tunable pore size, abundant metal active sites, large specific surface area, and excellent three-dimensional structural stability, many metal–organic frameworks (MOFs) are widely used in catalysis (Nunes et al. 2021; Shi et al. 2021; Silva et al. 2022; Souza et al. 2022), adsorption (Ahmed and Jhung 2014; Su et al. 2022a), drug delivery (Wang et al. 2022a), hydrogen storage (Elsabawy et al. 2022), sensing (Dong et al. 2021; Wang et al. 2022b), and other fields (Kim et al. 2017; Zhu and Xu 2014). Furthermore, MOF materials with tunable nanochannels can act as hosts to accommodate organic dye molecules as guests, constituting dye-encapsulated MOF composites with a wide range of applications in fluorescence sensing (Li et al. 2022a; Liu et al 2021; Wan et al. 2021; Xing et al. 2019), white light LEDs (Tang et al.2018), and nonlinear optics (Song et al. 2016). On the one hand, the encapsulation of dye molecules in MOF pores terminates the aggregation-induced quenching (ACQ) effect of the guest molecules and protects the guest against possible sources of degradation, thus stabilizing the optical signal output of the organic dyes (Let et al. 2020; Zhang et al. 2020). On the other hand, such dye-encapsulated MOF composites can be easily achieved simply by the "one-pot" or "post-synthesis modification" method and purified by convenient, low-cost routines such as filtration and centrifugation, improving the economics of the materials and paving the way for their application in optics-related fields (Let et al. 2020; Liu et al 2021). For applications in fluorescence sensing, since the additional fluorescence emission provided by the introduced dye can be used not only as a built-in reference, but also as a fluorescence response signal unit, the success of the dye-encapsulated MOF composites enriches the design concept of dual-emission ratiometric fluorescent probes and has become one of the most effective strategies for designing novel MOF-based ratiometric fluorescent probes (Li et al. 2022a; Wan et al. 2021; Yoo et al. 2019)

Recently, based on the conformational fixation induced luminescence enhancement of OTC, we have designed a rare-earth-free "turn-on" fluorescent probe for ultrasensitive detection of OTC, FMIL-53(Al), which is characterized by the abundant distribution of open aluminum sites on its surface that can coordinate with OTC molecules (Su et al. 2022b). Herein, based on the strategy of constructing dye-encapsulated MOF composites for ratiometric fluorescence sensing, by introducing blue-emitting fluorescent dye 2-aminoterephthalic acid (NH_2-BDC) (Figure S1 in supporting information) into the nanochannels of FMIL-53(Al), we constructed six NH_2-BDC@FMIL-53(Al) composites for OTC sensing, as illustrated in Scheme 1. Fortunately, under optimized sensing conditions, the prepared ratiometric fluorescent probe, NH_2-BDC@FMIL-53(Al)-3, retains the fluorescence enhancement response of the pristine MOF material to OTC at 520 nm, while the additional fluorescence emission intensity provided by the introduced dye does not fluctuate with the OTC concentration and can be used as a built-in reference. Meanwhile, the system showed an apparent fluorescent color change from blue to green under UV light at 365 nm. As for the analytical performance, the constructed ratiometric fluorescent probe can respond sensitively to OTC with a detection limit (LOD) of 11.01 nM, which was well below the maximum residue limits for tetracycline antibiotics in milk established by the European Union and the US Food and Drug Administration (225 nM and 676 nM, respectively). It is considered to be one of the most sensitive ratiometric fluorescent probes even when compared to currently reported probes for OTC ratiometric fluorescence sensing. Furthermore, the platform exhibits satisfactory reliabilities for detecting OTC in river water samples. In addition, portable test strips have been validated as a device for

rapid qualitative identification of OTC. More importantly, a smartphone-based sensing method for OTC detection was developed, providing a promising non-instrument-based technique for the reliable, semi-quantitative assay of OTC in the field. This work will provide a constructive strategy for the construction of rare-earth-free ratiometric fluorescence sensors for the highly sensitive detection of OTC.

Experimental

Fabrication of NH_2-BDC@FMIL-53(Al)

FMIL-53(Al) was prepared according to our previously reported solvothermal method (Su et al. 2022b). In brief, 10 mL of DMF solution dissolved with 1,4-dicarboxybenzene (PTA, 0.626 mmol, 104 mg) and acetic acid (17.5 mmol, 1 mL) were mixed with 5 mL of DMF solution dissolved with $AlCl_3{\cdot}6H_2O$ (1.0 *eqv*. 0.626 mmol, 151 mg) in a 50 mL scintillation vial. Subsequently, the mixture was transferred into a Teflon-lined steel autoclave and kept at 120 °C for 3 days. After cooling, the white crystals were obtained by centrifugation and then soaked in DMF for 3 days and ethanol for 24 h to remove impurities and DMF solvent molecules trapped in the pores, respectively, according to the reported method. Finally, the wet crystals were vacuum dried at 80 °C for 8 h to obtain FMIL-53(Al).

Six NH_2-BDC@FMIL-53(Al) composites were prepared by a post-synthetic modification method. Taking the preparation of NH_2-BDC@FMIL-53(Al)-3 as an example, 128 mg of FMIL-53(Al) was dissolved in 28.3 mL of NH_2-BDC solution (0.3 mM in absolute ethanol) and sonicated for 5 min at 25 ℃. Subsequently, the mixture was stirred for 6 h at 25 ℃ in the dark and then centrifuged (8500 rpm, 6 min). The obtained wet product was washed three times with absolute ethanol and vacuum dried at 80 °C overnight to obtain NH_2-BDC@FMIL-53(Al)-3.

By tuning the feeding concentration of NH_2-BDC solution in absolute ethanol from 0.2, 0.4, 0.5 to 0.6 mM, other dye-encapsulated MOF composites, i.e., NH_2-BDC@FMIL-53(Al)-1, NH_2-BDC@FMIL-53(Al)-2, NH_2-BDC@FMIL-53(Al)-4, NH_2-BDC@FMIL-53(Al)-5, and NH_2-BDC@FMIL-53(Al)-6 were also successfully synthesized by the same procedure. By comparing the concentration of NH_2-BDC in the supernatant before and after the preparation of dye-encapsulated MOF composites, the contents of the dye in NH_2-BDC@FMIL-53(Al)-1, NH_2-BDC@FMIL-53(Al)-2, NH_2-BDC@FMIL-53(Al)-3, NH_2-BDC@FMIL-53(Al)-4, NH_2-BDC@FMIL-53(Al)-5, and NH_2-BDC@FMIL-53(Al)-6 composites were calculated to be 0.173, 0.568, 0.861, 1.157, 1.375, and 1.66 wt%, respectively (Table S1 in supporting information).

Fluorescence detection of OTC

By introducing the prepared NH_2-BDC@FMIL-53(Al)-3 powder (15.0 mg) into 7.5 mL of 10 mM HEPES buffer (pH = 7.3) and dispersing by sonication for 30 min at 25 ℃, the uniform dispersed MOF-based probe suspension was firstly prepared. For fluorescence titration experiments, 2 mL of HEPES buffer (pH = 7.3), 150 μL of well-mixed probe suspension, and different volumes (0, 3, 9, 15, 24, 30, 39, 45, 54, 60, 75, 90, and 120 μL, respectively) of 0.1 mM OTC solutions were sequentially added into the sequentially numbered centrifuge tubes. The mixtures were diluted to a final volume of 3.0 mL with 10 mM HEPES buffer (pH = 7.3), followed by incubating for 45 min at 25 ℃ in the dark. Finally, the OTC-NH_2-BDC@FMIL-53(Al)-3 systems were mixed uniformly, and the spectra were recorded with the excitation wavelength of 383 nm and the scan rate of 1200 nm/min at room temperature.

Selectivity and interference experiments

For the selective experiments, 150 μL of well-mixed probe suspension and 450 μL of each interfering compound (including streptomycin sulfate (SMC), secnidazole (SDZ), kanamycin sulfate (KNMC), norfloxacin (NFX), erythromycin (Eryc), chloramphenicol (CAP), ceftriaxone sodium (CTA), ampicillin (APCL), nitrofurazone (NFZ), Ca^{2+}, Ba^{2+}, Mg^{2+}, Fe^{3+}, K^+, NH_4^+, Ni^{2+}, Na^+, Cu^{2+}, Cl^-, NO_3^-, CO_3^{2-}, HCO_3^-, $H_2PO_4^-$, HPO_4^{2-}, SO_4^{2-}, and $S_2O_3^{2-}$) solution with the concentration of 0.1 mM were added to 2.4 mL HEPES buffer (10 mM, pH = 7.3). Besides, to verify the anti-interference capability of the ratiometric fluorescent sensor to OTC, 90 μL of the OTC solution (0.1 mM) and 450 μL of each interfering substance with a concentration of 0.1 mM were added to a mixture of 150 μL of well-mixed NH_2-BDC@FMIL-53(Al)-3 suspension and 2.31 mL of HEPES buffer (10 mM, pH = 7.3). Finally, all samples were incubated and fluorescence measured following the steps described above.

Determination of OTC in real samples

From a local river in *Maoming*, *Guangdong*, *China*, the river water samples were sampled and, then, filtered through a 0.22 μm membrane before use. Subsequently, spiked samples containing 40 μM and 80 μM OTC were accurately prepared by the standard addition method. Finally, the content

of OTC in the spiked samples was quantified according to the procedure mentioned above. To determine intra-day and inter-day precision, for the spiked samples, four repetitive analyses in a single day and duplicate analysis on four successive days were performed, respectively.

Paper sensors based on NH_2-BDC@FMIL-53(Al) for OTC

Typically, dispersed 10.0 mg NH_2-BDC@FMIL-53(Al)-3 into 5.0 mL EtOH and treated with ultrasonication for at least 45 min to form MOF-based probe suspension. Then, dropped 20 µL of the well-mixed probe suspension onto a 6 mm diameter round glass fiber filter paper with a diameter of 6 mm, and subsequently air dried at room temperature in the dark to form a test strip. For the visual detection of OTC, 20 µL of OTC solutions (5 µM, 10 µM, 15 µM, 20 µM, 25 µM, and 30 µM) were added directly onto the center of the test strips. After drying for 2 h at room temperature under vacuum conditions, the fluorescence color of the test strips was observed and photographed under the excitation of 365 nm ultraviolet light.

Results and discussion

Rational design of NH_2-BDC@FMIL-53(Al) for ratiometric fluorescence sensor

Although a single-color fluorescence-based rare-earth-free probe was reported previously for OTC detection based on "turn-on" fluorescence using surface-wrinkled MIL-53(Al) (Su et al. 2022b), the two-color fluorescence signal-based ratiometric fluorescence method provides built-in correction for external interference and its continuous color change upon addition of the analyte(s) offers the possibility of fast visual identification. Therefore, we considered the introduction of dye molecules as built-in signal molecules within the pores of the MOF to construct a novel rare-earth-free ratiometric fluorescent probe for sensitive ratiometric sensing of OTC. Recognizing that the pore diameter of FMIL-53(Al) is about 0.5 nm, we designed the ratiometric fluorescence sensor NH_2-BDC@FMIL-53(Al) by selecting a 2-aminoterephthalic acid (NH_2-BDC) dye with a suitable size and capable of emitting blue fluorescence and introducing it into the pores of FMIL-53(Al) (Scheme 1 and Figure S1 in supporting information). Besides, in contrast to the "one-pot" method of preparing dye-embedded MOF complexes, the amount of dye in dye-encapsulated MOF composites prepared by "post-synthetic modification" method can be easily quantified by UV spectroscopy. Thus, the method of post-synthesis modification was chosen herein for the preparation of dye-embedded MOF composites.

Material synthesis and characterization

FMIL-53(Al) was firstly prepared by solvothermal reaction between $AlCl_3 \cdot 6H_2O$ and terephthalic acid (PTA) at 120 °C for 72 h. To investigate the optimal reaction time for the preparation of NH_2-BDC@FMIL-53(Al) composites, the adsorption of NH_2-BDC in FMIL-53(Al) was traced by UV spectroscopy. As shown in Figure S4 in supporting information, a rapid adsorption occurred in the first 35 min and the equilibrium was reached within 6 h. Six NH_2-BDC@FMIL-53(Al) composites were obtained by stirring FMIL-53(Al) particles in an ethanolic solution of NH_2-BDC for 6 h at room temperature. By the way, two kinetic models (pseudo-first-order model and pseudo-second-order model) were tested to fit the kinetic data. The higher R^2 value ($R^2 = 0.9999$) indicates that the pseudo-second-order model fits the kinetic data well, indicating the chemical adsorption process and non-diffusion controlled processes (Figure S5 in supporting information) (Sun et al. 2020a).

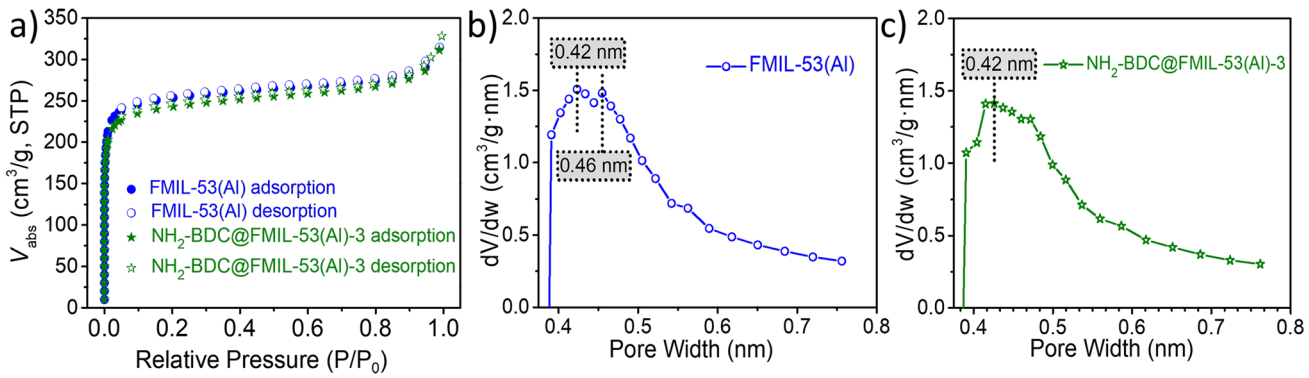

Fig. 1 **a** N_2 adsorption/desorption isotherms of FMIL-53(Al) and NH_2-BDC@FMIL-53(Al)-3, respectively, at 77 K. DFT pore size distribution for **b** FMIL-53(Al) and **c** NH_2-BDC@FMIL-53(Al)-3 evaluated by using N_2 adsorption data measured at 77 K

Furthermore, as a representative of the six NH_2-BDC@FMIL-53(Al) composites, the NH_2-BDC@FMIL-53(Al)-3 was characterized by powder X-ray diffraction (PXRD), Brunauer–Emmett–Teller (BET) measurements, scanning electron micrograph (SEM), and thermogravimetric analysis (TGA). As shown in Fig. 1a, both the N_2 adsorption–desorption isotherms of FMIL-53(Al) and NH_2-BDC@FMIL-53(Al)-3 can be classified as type-I isotherms. As expected, the Brunauer–Emmett–Teller areas (A_{BET}) of NH_2-BDC@FMIL-53(Al)-3 is 755.63 $m^2\ g^{-1}$, which is slightly smaller than that of FMIL-53(Al)(787.12 $m^2\ g^{-1}$) due to the loading of NH_2-BDC molecules. Furthermore, the pore size distributions of FMIL-53(Al) before and after NH_2-BDC loaded were calculated by the DFT (density function theory) model, which gave two types of pores of 0.42 and 0.46 nm for FMIL-53(Al) but one type of pore of 0.42 nm for NH_2-BDC@FMIL-53(Al)-3, indicating the loaded NH_2-BDC molecules were successfully trapped into the nanochannels of FMIL-53(Al) (Fig. 1b, c).

Morphology of NH_2-BDC@FMIL-53(Al)-3 composites was studied by SEM. As shown in Fig. 2, NH_2-BDC@FMIL-53(Al)-3 exhibits a surface-wrinkled microflower-like morphology similar to the pristine MOF material (Su et al. 2022b). Furthermore, the PXRD patterns of NH_2-BDC@FMIL-53(Al)-3 showed the same characteristic peaks of FMIL-53(Al), which also implied that the crystal structure of FMIL-53(Al) remained stable during the dye loading (Figure S3 in supporting information). Finally, the TG experimental results showed almost no mass loss of the material in the range less than 300 °C, indicating the high thermal stability of NH_2-BDC@FMIL-53(Al)-3 (Figure S2 in supporting information). In the range of 300–520 °C, there is a continuous weight loss (~ 15% weight loss) due to the release of guest molecules, such as DMF and NH_2-BDC molecules. Continuing to increase the temperature, a rapid and significant mass loss was observed due to the collapse of the FMIL-53(Al) framework structure and the decomposition of the PTA ligand.

Response of the fabricated ratiometric probe to OTC

The fluorescence characteristic peak of six NH_2-BDC@FMIL-53(Al) composites, as shown in Figure S6 in supporting information, clearly appeared at about 433 nm due to the introduction of blue fluorescent dye. In addition, the fluorescence intensity at 433 nm gradually increased with the increase in NH_2-BDC content in NH_2-BDC@FMIL-53(Al) composites. Considering the fluorescence enhancement response of FMIL-53(Al) to OTC, NH_2-BDC@FMIL-53(Al)-3, which has moderate intensity fluorescence emission at 433 nm and 520 nm, was chosen as the fluorescence sensor for ratiometric sensing of OTC. The addition of 4.0 μM OTC can significantly (about 13-fold) enhance the emission of green emission (F_G) under excitation at a single wavelength of 383 nm, while the intensities of blue-emitting (F_B) centered at 433 nm almost kept constant (Figure S18 in supporting information). Hence, NH_2-BDC@FMIL-53(Al)-3 can be developed as a ratiometric fluorescent probe for OTC detection, in which FMIL-53(Al) can act as a reactive component specific to OTC and leads to the enhancement of green fluorescence, while NH_2-BDC can serve as a reference signal.

Optimization of sensing conditions

Keeping stability in mind as a prerequisite for material applications (Lima et al. 2017; Liu and Dong 2020; Sanchez et al. 2016; Zahirinejad et al. 2021), the fluorescence stability of NH_2-BDC@FMIL-53(Al)-3 was first verified in organic solvents (DMF, acetone, DCM, THF, ethanol, ethyl acetate, propan-2-ol, and *n*-Hexane), HEPES buffer (10 mM, pH = 7.3), metal ion (K^+, Na^+, Zn^{2+}, and Ca^{2+}), and surfactant (CTAB and SDS) solutions. As shown in Figure S7 and Figure S8 in supporting information, the blue emission of NH_2-BDC@FMIL-53(Al)-3 remained almost constant over 3 days, indicating that NH_2-BDC@FMIL-53(Al)-3 possesses sufficient fluorescence stability under the above media conditions. In addition, we examined the effect of pH on the fluorescence of the probe. NH_2-BDC@FMIL-53(Al)-3 also

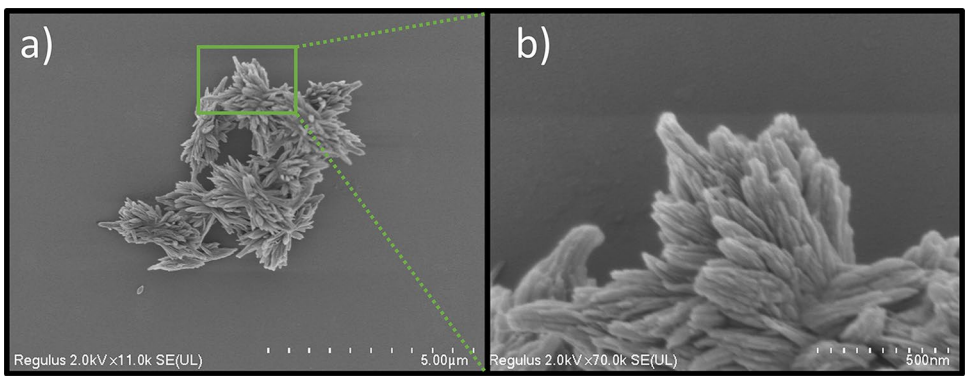

Fig. 2 SEM images of NH_2-BDC@FMIL-53(Al)-3 at two scales: **a**. 5.0 μm, **b** 500 nm

exhibited satisfactory luminescence stability with the solution in the pH range of 5.0–9.0 (Figure S10 in supporting information). Next, we explored the fluorescence response of the probe to OTC in organic solvents and HEPES buffer. Only in HEPES buffer, NH_2-BDC@FMIL-53(Al)-3 exhibited a ratiometric fluorescence response to OTC (Figure S9 and Figure S18 in Supporting information). Thus, HEPES buffer was chosen as the medium for OTC sensing. Furthermore, the effect of pH on OTC sensing was also explored in the buffer range (pH = 6.8–8.2) of HEPES buffer. According to the result in Figure S14 in supporting information, the sensing efficiency did not exhibit significant pH-dependent properties.

In addition, the effect of response time was next investigated. With the addition of OTC, the ratiometric probe-OTC system exhibited time-dependent spectral characteristics, and the signal of F_G/F_B showed a significant enhancement effect within 45 min (Figure S13 in supporting information). Finally, as a non-negligible factor, the optimal excitation wavelength in the sensing process was also investigated in detail. Specifically, after adding different concentrations of OTC from 1.0 to 4.0 μM, the fluorescence emission spectrum of the ratiometric probe-OTC system excited at different excitation wavelengths (370 nm, 375 nm, 380 nm, 383 nm, and 385 nm) was recorded (Figures S15-S19 in supporting information). Taking the addition of 4.0 μM OTC as an example, with the increase in the excitation wavelength from 370 to 385 nm, the green emission of the ratiometric probe-OTC system was enhanced by 4.8, 6.4, 9.6, 13.0 and 15.2 times, respectively. However, the blue emission intensity, which can be used as an internal standard, remained stable only when the excitation wavelength was 383 nm. Therefore, 383 nm was chosen as the optimal excitation wavelength for OTC detection.

Sensing mechanism

In addition, we speculated the possible mechanism of NH_2-BDC@FMIL-53(Al) response to OTC molecules. Typically, in neutral solutions, OTC molecules adopt a twisted conformation with weak/no fluorescence (Fig. 3b) (Carlotti et al. 2012; Lambs et al. 1988). While the coordination with metal ions such as Ca^{2+}, Zn^{2+}, or Al^{3+} can promoted conformation of the OTC molecules gradually evolves from a twisted conformation to an extended conformation, accompanied by an intense yellow-green fluorescence emission and a clear red shift of the absorption peak (Carlotti et al. 2012; Lambs et al. 1988). We have elucidated that the OTC molecules can bind to FMIL-53(Al)'s surface-distributed open aluminum sites, which promotes the evolution of OTC molecules to an extended conformation, as evidenced by enhanced green emission intensity and redshifted absorption peaks (Su et al. 2022b). Here, the NH_2-BDC@FMIL-53(Al)-OTC system exhibits similar spectral phenomena, including the enhancement of the fluorescence at ~ 520 nm and the redshift of the UV–vis absorption (Fig. 3a and Figure S18 in supporting information). Furthermore, as shown in Fig. 3a and Figure S11 in supporting information, EDTA, a common metal ion chelator, can significantly interfere with the interaction of OTC molecules with the probe, as reflected in the fluorescence and absorption spectra of the Probe-EDTA-OTC ternary system. Those results demonstrated the interaction between OTC molecules and the surface-distributed open aluminum sites. Thus, similar to the pristine MOF material, the mechanism by which the constructed ratiometric fluorescent probe enhances the fluorescence of OTC molecules can also be described as the conformational change driven by the coordination to NH_2-BDC@FMIL-53(Al)'s surface-distributed open aluminum sites.

In addition, the reusability of functional materials is an important characteristic, which is considered as a continuous application (Galvão et al. 2018; Pinheiro et al. 2018). To investigate the reusability of the probe, after the detection

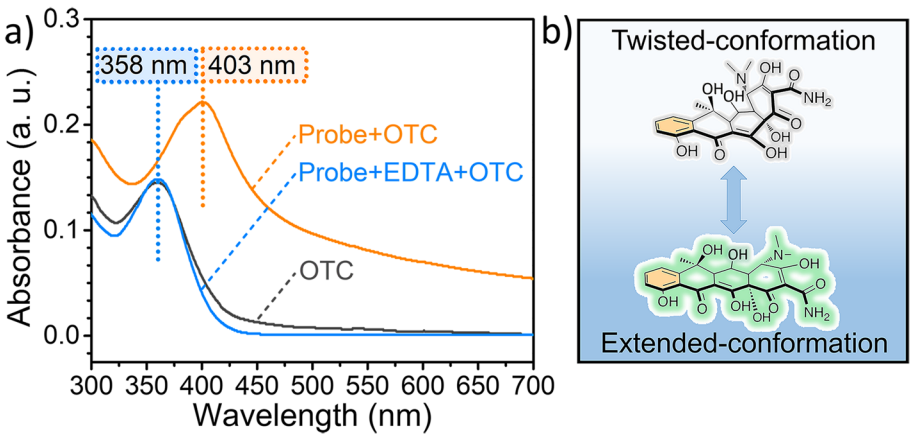

Fig. 3 **a** Absorption spectra of OTC (10 μM) with (Orange) or without (black) the addition of the probe, and the probe-EDTA system with the addition of 10 μM OTC (blue) in HEPES buffer. The concentrations of EDTA and probe were 500 μM and 0.1 mg/mL. **b** The balance between the twisted conformation and the extended conformation

of OTC, used FMIL-53(Al), noted as OTC@NH_2-BDC@FMIL-53(Al)-3, was first obtained by centrifugation and vacuum drying. Next, OTC@NH_2-BDC@FMIL-53(Al)-3 solids were treated by immersion in ethanol for different times (0 h, 2 h, 4 h, and 6 h) and then redispersed in HEPES buffer, and the fluorescence spectra were recorded with the excitation wavelength of 383 nm. As shown in Figure S12 in supporting information, the fluorescence intensity at 520 nm did not decrease significantly with the extension of soaking time, indicating the poor recoverability of the probe, which also briefly demonstrated the strong binding between the OTC and the open aluminum sites on the surface of FMIL-53(Al).

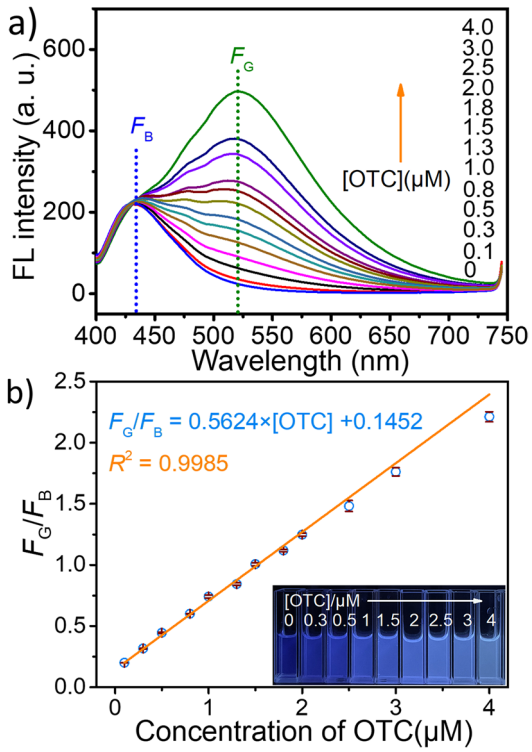

Fig. 4 **a** Dose-dependent response of the fluorescence spectra (λ_{ex} = 383 nm) of NH_2-BDC@FMIL-53(Al)-3 (0.1 mg mL^{-1}) under various concentrations of OTC: 0, 0.1, 0.3, 0.5, 0.8, 1.0, 1.3, 1.5, 1.8, 2.0, 2.5, 3.0, and 4.0 μM. **b** Standard curve for the determination of OTC concentration. Calibration curve of F_G/F_B versus concentration of OTC from 0.1 to 4.0 μM. (inset) Photographs depicting OTC-induced ratiometric fluorescence change from dark blue to steel blue under UV light at 365 nm. The error bars are the standard deviations (n = 3) calculated based on the results of triplicate trials

Fluorescence titration experiments

The dose-dependent response of prepared probe to OTC was examined by fluorescence titration experiments. When exposed to OTC, the green fluorescence centered at ~ 520 nm gradually increased, whereas the blue fluorescence at 433 nm of NH_2-BDC as an internal standard remains unchanged (Fig. 4a). A well linear response (R^2 = 0.9985) between the value of F_G/F_B and the concentration of OTC (0–4.0 μM) can be fitted as a regression equation of F_G/F_B = 0.5624 × [OTC] + 0.1452, where F_G/F_B is the ratios of the intensities of green fluorescence (F_G) to the intensities of blue fluorescence (F_B), and [OTC] represents the concentration of OTC (Fig. 4b). Correspondingly, the limit of detection (LOD) and limit of quantitation (LOQ) were calculated by 3σ/S (Güner et al. 2022; Turan et al. 2019) and 10σ/S (Güner et al. 2022; Turan et al. 2019) to be 11.0 nM and 36.70 nM, respectively, which were well below the maximum residue limits for tetracycline antibiotics in milk established by the European Union and the US Food and Drug Administration (225 nM and 676 nM, respectively) (Li et al. 2019). More importantly, as shown in Table 1, NH_2-BDC@FMIL-53(Al)-3 exhibits high sensitivity, which is comparable to the most sensitive ratiometric fluorescent probes reported for OTC detection. Furthermore, under the excitation of 365 nm UV light, against the background of blue fluorescence of stable intensity, the enhancement of green fluorescence resulted in

Table 1 Comparison of ratiometric fluorescent sensors for OTC detection

Complex	Sensing medium	Response time	Detection limit	References
NH_2-BDC@FMIL-53(Al)-3	HEPES buffer	45 min	11.0 nM	This work
CD@AMP/Eu NCPs	Water	3 min	25 nM	Chen et al. (2020a)
BNQD-Eu^{3+}	Water	3 min	0.104 μM	Yang et al. (2021)
CDs@HZIF-8	Tris–HCl buffer	1 min	29.46 nM	Li et al. (2022b)
GQDs/CdTe@MIPs	Water	10 min	3.5 nM	Wang et al. (2020)
CDs	K_2HPO_4–NaOH buffer	1 min	0.41 μM	Fu et al. (2021)
FHBA@ZIF-8@Eu-GMP	HEPES buffer	5 min	30 nM	Sun et al. (2022)
Tb-L1	Water	–	20 ng/mL[43 nM]	Li et al. (2021)
S, N-CDs	PBS buffer	30 s	0.26 μM	Xing et al. (2020)
TA-CuNCs-Eu^{3+}	HEPES buffer	3 min	15 nM	Mo et al. (2022)
SiNPs	Water	2 min	0.18 μM	Xu et al. (2017)

a continuous evolution of fluorescence color from dark blue to steel blue with the addition of 4.0 μM OTC (Fig. 4b inset).

Selectivity and interference studies

To determine the specificity of the prepared ratiometric fluorescent probe toward OTC, other relevant antibiotics (including Eryc, KNMC, CAP, SMC, SDZ, NFX, CTA, APCL, and NFZ), metal ions (including Ca^{2+}, Zn^{2+}, Mn^{2+}, Al^{3+}, Ni^{2+}, Co^{2+}, K^{+}, and Na^{+}), and anions (including Cl^{-}, Br^{-}, I^{-}, NO_2^{-}, CO_3^{2-}, HCO_3^{-}, HPO_4^{2-}, S^{2-}, SO_4^{2-}, IO_3^{-}, and Ac^{-}), each at a concentration of 15 μM, were added to the NH_2-BDC@FMIL-53(Al)-3 suspension and fluorescence spectra were recorded, respectively. As can be seen from Fig. 5, compared to the intensity ratio $(F_G/F_B)_0$ of the blank sample without analyte added, the addition of these foreign species did not cause significant changes in the intensities ratios F_G/F_B, while 3 μM OTC could lead to a ~ 12-fold increase in the F_G/F_B ratio, demonstrating the high selectivity toward OTC. Furthermore, the effects of the coexistence of the above-mentioned species on the ratiometric fluorescent probe for OTC sensing were verified. The results showed that 5 times the concentration of coexisting antibiotics, metal ions, or anions did not significantly interfere with the sensing of OTC, which further verified the feasibility of the proposed ratiometric probe (Fig. 6).

Detection of OTC in river water samples

We further evaluated the practicability of the proposed ratiometric fluorescence method for OTC detection based on NH_2-BDC@FMIL-53(Al)-3, and the river water samples were selected for spike and recovery tests (Chen et al. 2020b; Sun et al. 2020b). As listed in Table 2, the relative recoveries (99.8% – 102.6%) on river water samples with 2.0 and 4.0 μM of OTC spiked were obtained with low relative standard deviation (RSD, $n = 3$) values of

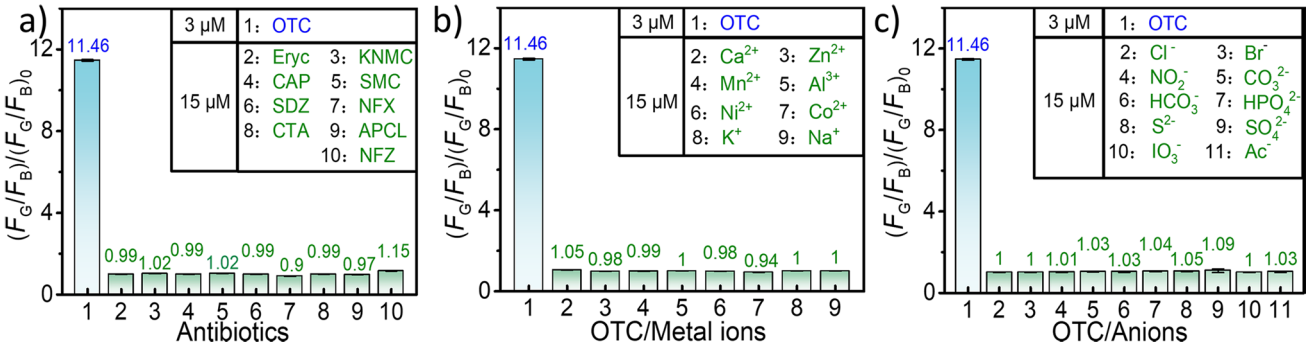

Fig. 5 The fluorescence ratiometric selectivity of NH_2-BDC@FMIL-53(Al)-3 to **a** interfering antibiotics, **b** interfering metal ions, and **c** interfering anions. $(F_G/F_B)_0$ and (F_G/F_B) were the ratios of the intensities of green fluorescence (F_G) to the intensities of blue fluorescence (F_B) without and with analytes, respectively. The error bars are the standard deviations ($n = 3$) calculated based on the results of triplicate trials

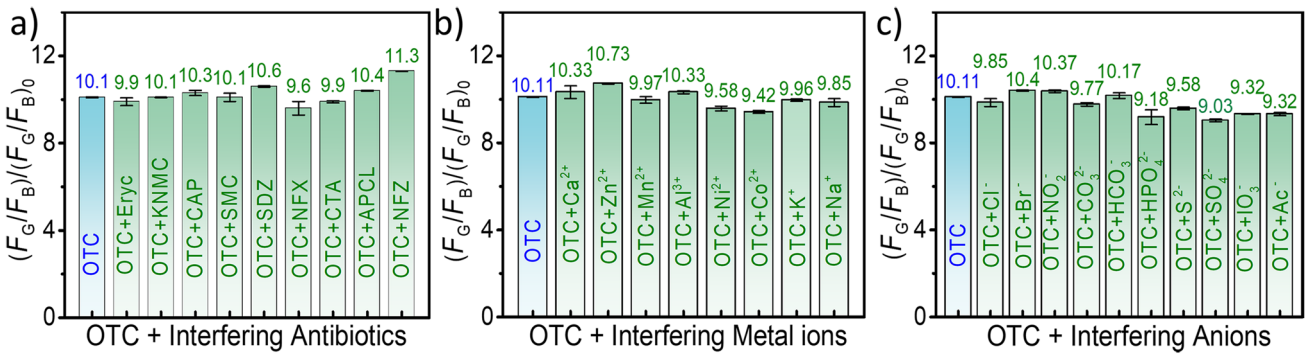

Fig. 6 Fluorescence intensities ratio of $(F_G/F_B)/(F_G/F_B)_0$ from the responses of NH_2-BDC@FMIL-53(Al)-3 in the presence of 3 μM OTC coexisting with 15 μM **a** interfering antibiotics, **b** interfering metal ions, and **c** interfering anions. $(F_G/F_B)_0$ and (F_G/F_B) were the ratios of the luminescence intensities without and with the analytes, respectively. The error bars are the standard deviations ($n = 3$) calculated based on the results of triplicate trials

Table 2 Determination of OTC in ultrapure water and river water samples by NH_2-BDC@FMIL-53(Al)-3 nanoprobe

Spiked (μM)	Ultrapure water		River water	
	Found (μM)	Relative recovery ± RSD % (n = 3)	Found (μM)	Relative recovery ± RSD % (n = 3)
2.0	2.006	100.3 ± 0.27	2.052	102.6 ± 0.91
4.0	3.972	99.3 ± 0.24	3.992	99.8 ± 0.35

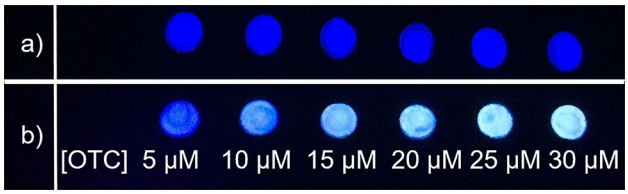

Fig. 7 Photographs depicting the test strips **a** before and **b** after sensing of OTC solutions under a 365 nm UV lamp. The concentrations of OTC were 5 μM, 10 μM, 15 μM, 20 μM, 25 μM, and 30 μM from left to right

0.35–0.91%. In addition, compared with the measurement results in ultrapure water, no obvious matrix effect was found, indicating that the sensing process was not seriously interfered with by the environmental substances in real river water (Table S2 in supporting information). The relative recoveries obtained in real and ultrapure water samples were also statistically analyzed by applying t test, and no significant differences were noticed, as shown in Table S2 in supporting information. Furthermore, the analytical precision (intra-day and inter-day) of this ratiometric fluorescence method was calculated from real samples spiked with 2.0 μM and 4.0 μM OTC. As shown in Table S3 in supporting information, the intra-day and inter-day RSDs (n = 4) were within the ranges 0.55–1.39% and 0.95–1.26%, respectively, indicating the reliability of the probe for OTC quantification. All those results confirmed that the prepared ratiometric fluorescence sensing approach possessed practicability and reliability for quantification of OTC in real samples.

Paper-based method for visual detection of OTC

To further explore such OTC-triggered ratiometric fluorescence response for real-time monitoring, the circular test strips with a diameter of 6 nm were firstly prepared by loading NH_2-BDC@FMIL-53(Al)-3 on glass fiber filter paper. The test strips loaded with ratiometric fluorescent probes showed no obvious change under sunlight but emitted strong blue light under the irradiation of a hand-held UV 365 nm lamp (Figure S20 in supporting information). For application in visual detection, 20 μL of different concentrations of OTC (5 μM, 10 μM, 15 μM, 20 μM, 25 μM, and 30 μM) were sequentially dropped on the test strips, followed by vacuum drying at room temperature for 30 min. Under 365 nm ultraviolet light, the test strips showed a concentration-dependent yellow patch against the blue fluorescent background, which could be identified by the naked eye conveniently (Figs. 7b). Therefore, the above results demonstrate that the developed test strips can achieve rapid and simple detection of OTC.

Smartphone application used to detect OTC

As mentioned above, the ratiometric fluorescence method based on NH_2-BDC@FMIL-53(Al)-3 can realize sensitive sensing of OTC, but the detection process involves the use of an expensive and bulky fluorophotometer, which is not suitable for field application. In addition, the paper-based method for visual detection can quickly and easily detect OTC, but it is difficult to accurately quantify the OTC concentration due to the inability of the naked eye to distinguish subtle color changes. To make the proposed ratiometric probe available for accurate on-site monitoring of OTC, a non-instrument-based semi-quantitative analysis method was established based on the color recognizer APP in the smartphone application (Fig. 8a and Figure S21 in supporting information). Specifically, the color recognizer APP was used as a signal reader to digitize the color information (RGB values) of the fluorescent color image shown in the inset of Fig. 4b, and the correlation between the RGB ratios (G/B) and the OTC concentration was calculated and fitted. As illustrated in Fig. 8b, within the concentration ranging from 0.3 to 4.0 μM, the RGB ratio (G/B) has a favorable linear correlation with the OTC concentration (R^2 = 0.9956). The corresponding linear equation can be expressed by $G/B = 0.1114 \times [\text{OTC}] + 0.2673$, while the lowest detectable concentration was estimated to be 0.18 μM. Therefore, the above experimental results demonstrate the reliability of the smartphone-based sensing method for OTC detection, validating the applications of the fabricated NH_2-BDC@FMIL-53(Al)-3 composites for point-of-care analysis of OTC.

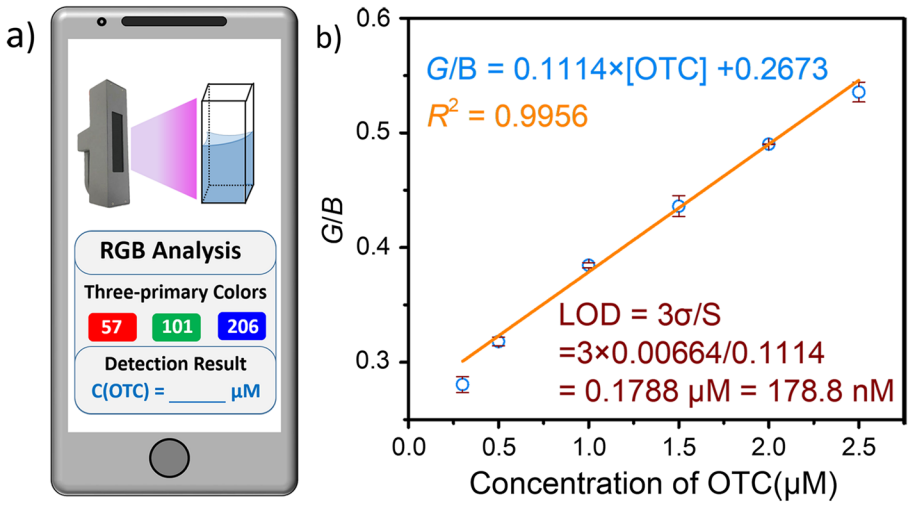

Fig. 8 **a** Schematic diagram of digitizing RGB values of fluorescent photos via smartphone color recognizer. **b** Favorable Linear relationship plots of RGB ratios (*G*/*B*) versus OTC concentrations (OTC concentrations: 0.3 μM, 0.5 μM, 1.0 μM, 1.5 μM, 2.0 μM, and 2.5 μM). The error bars are the standard deviations ($n = 3$) calculated based on the results of triplicate trials

Conclusions

In conclusion, six NH_2-BDC@FMIL-53(Al)-based rare-earth-free composites for ratiometric fluorescence sensing of OTC were fabricated by introducing blue-emitting fluorescent dye 2-aminoterephthalic acid (NH_2-BDC) into the nanochannels of FMIL-53(Al). The detection limit (LOD) and quantitation limit (LOQ) of NH_2-BDC@FMIL-53(Al)-3 are estimated to be as low as 11.01 nM and 36.70 nM, respectively, which is considered to be one of the most sensitive ratiometric fluorescent probes for OTC detection. In contrast to most rare-earth element containing probes, it is important to emphasize that the ratiometric fluorescent probes NH_2-BDC@FMIL-53(Al) composites we constructed do not contain rare-earth elements, which implies low cost, abundant supply, and environmental friendliness. More importantly, the continuous color evolution caused by the addition of OTC can be recognized by the color identifier APP in the smartphone application, enabling quantitative detection of OTC with a LOD of 0.18 μM. Finally, OTC in river water samples can also be quantified, demonstrating the application potential of the constructed ratiometric fluorescence sensing platform.

Supplementary Information The online version contains supplementary material available at https://doi.org/10.1007/s11696-022-02629-8.

Acknowledgements We acknowledge the financial support from the National Natural Science Foundation of China (U21A20290, 22176044), the Guangdong Basic and Applied Basic Research Foundation (2022A1515011656), Guangdong Provincial Special Funding projects for Introducing Innovation Team and Industry University Research Cooperation (2019C002001).

Author contributions PS contributed to methodology, investigation, data curation, and writing—original draft. LY contributed to methodology and investigation. MY contributed to supervision, methodology, and software. LW contributed to methodology and investigation. MS contributed to methodology. HT contributed to investigation. WH contributed to investigation. SW contributed to supervision and writing—review and editing.

Data availability All data generated or analyzed during this study are included in this published article and its supplementary information files.

Declarations

Conflict of interest The authors declare that they have no competing interests.

References

Ahmed I, Jhung SH (2014) Composites of metal–organic frameworks: preparation and application in adsorption. Mater Today 17(3):136–146. https://doi.org/10.1016/j.mattod.2014.03.002

Anadón A, Rodriguez JL, Fernández C, Carbonell G, Pro J (2016) Oxytetracycline effects in aquatic and terrestrial biotic systems. Toxicol Lett 258:S226–S227. https://doi.org/10.1016/j.toxlet.2016.06.1814

Carlotti B, Cesaretti A, Elisei F (2012) Complexes of tetracyclines with divalent metal cations investigated by stationary and femtosecond-pulsed techniques. Phys Chem Chem Phys 14:823–834. https://doi.org/10.1039/C1CP22703C

Chen Y, Kong D, Liu L, Song S, Kuang H, Xu C (2016) Development of an ELISA and immunochromatographic assay for tetracycline, oxytetracycline, and chlortetracycline residues in milk and honey based on the class-specific monoclonal antibody. Food Anal Methods 9:905–914. https://doi.org/10.1007/s12161-015-0262-z

Chen L, Xu H, Wang L, Li Y, Tian X (2020a) Portable ratiometric probe based on the use of europium(III) coordination polymers doped with carbon dots for visual fluorometric determination of oxytetracycline. Microchim Acta 187:125. https://doi.org/10.1007/s00604-019-4104-3

Chen H, Peng J, Yu L, Chen H, Sun M, Sun Z, Ni R, Alamry KA, Marwani HM, Wang S (2020b) Calcium ions turn on the fluorescence

of oxytetracycline for sensitive and selective detection. J Fluoresc 30:463–470. https://doi.org/10.1007/s10895-020-02512-3

da Souza JES, de Oliveira GP, Alexandre JYNH, Neto JGL, Sales MB, de Junior PGS, de Oliveira ALB, de Souza MCM, dos Santos JCS (2022) A comprehensive review on the use of metal-organic frameworks (MOFs) coupled with enzymes as biosensors. Electrochem 3(1):89–113. https://doi.org/10.3390/electrochem3010006

Dong C, Li M, Yang T, Feng L, Ai Y, Ning Z, Liu M, Lai X, Gao D (2021) Controllable synthesis of Tb-based metal–organic frameworks as an efficient fluorescent sensor for Cu_2^+ detection. Rare Met 40:505–512. https://doi.org/10.1007/s12598-020-01621-z

Elsabawy KM, Fallatah AM, Owidah ZO (2022) Synthesis of newly crystalline-porous-Pd(II)-(*E*, *E*)-2, 4-hexadienoic acid complex-leads to 3D-MOFs for hydrogen storage. J Mol Struct 1250(1):131723. https://doi.org/10.1016/j.molstruc.2021.131723

Esmaelpourfarkhani M, Abnous K, Taghdisi SM, Chamsaz M (2019) A fluorometric assay for oxytetracycline based on the use of its europium(III) complex and aptamer-modified silver nanoparticles. Microchim Acta 186:290. https://doi.org/10.1007/s00604-019-3389-6

Fu Y, Huang L, Zhao S, Xing X, Lan M, Song X (2021) A carbon dot-based fluorometric probe for oxytetracycline detection utilizing a Förster resonance energy transfer mechanism. Spectrochim Acta Part A 246:118947. https://doi.org/10.1016/j.saa.2020.118947

Gajda A, Jablonski A, Bladek T, Posyniak A (2017) Oral fluid as a biological material for antemortem detection of oxytetracycline in pigs by liquid chromatography-tandem mass spectrometry. J Agric Food Chem 65:494–500. https://doi.org/10.1021/acs.jafc.6b05205

Galvão WS, Pinheiro BBL, Golçalves RB, de Mattos MC, Fonseca TS, Regis T, Zampieri D, dos Santos JCS, Costa LS, Correa MA, Bohn F, Fechine PBA (2018) Novel nanohybrid biocatalyst: application in the kinetic resolution of secondary alcohols. J Mater Sci 53:14121–14137. https://doi.org/10.1007/s10853-018-2641-5

Güner D, Sener BB, Bayrac C (2022) Label free detection of auramine O by G-quadruplex-based fluorescent turn-on strategy. Spectrochim Acta Part A 267:120532. https://doi.org/10.1016/j.saa.2021.120532

Kim JY, Zhang L, Balderas-Xicohténcatl R, Park J, Hirscher M, Moon HR, Oh H (2017) Selective hydrogen isotope separation via breathing transition in MIL-53(Al). J Am Chem Soc 139(49):17743–17746. https://doi.org/10.1021/jacs.7b10323

Kuong CL, Yu TJ, Chen YC (2009) Microwave-assisted sensing of tetracycline using europium-sensitized luminescence fibers as probes. Anal Bioanal Chem 395:1433–1439. https://doi.org/10.1007/s00216-009-3106-0

Lambs L, Reverend BDL, Kozlowski H, Berthon G (1988) Metal ion-tetracycline interactions in biological fluids. 9. Circular dichroism spectra of calcium and magnesium complexes with tetracycline, oxytetracycline, doxycycline, and chlortetracycline and discussion of their binding Modes. Inorg Chem 27:3001–3012. https://doi.org/10.1021/ic00290a022

Let S, Samanta P, Dutta S, Ghosh SK (2020) A Dye@MOF composite as luminescent sensory material for selective and sensitive recognition of Fe(III) ions in water. Inorg Chim Acta 500:119205. https://doi.org/10.1016/j.ica.2019.119205

Li C, Zhu L, Yang W, He X, Zhao S, Zhang X, Tang W, Wang J, Yue T, Li Z (2019) Amino-functionalized Al−MOF for fluorescent detection of tetracyclines in milk. J Agric Food Chem 67(4):1277–1283. https://doi.org/10.1021/acs.jafc.8b06253

Li C, Zeng C, Chen Z, Jiang Y, Yao H, Yang Y, Wong WT (2020a) Luminescent lanthanide metal-organic framework test strip for immediate detection of tetracycline antibiotics in water. J Hazard Mater 384:121498. https://doi.org/10.1016/j.jhazmat.2019.121498

Li C, Zhang X, Wen S, Xiang R, Han Y, Tang W, Yue T, Li Z (2020b) Interface engineering of zeolite imidazolate framework-8 on twodimensional Al-metal-organic framework nanoplates enhancing performance for simultaneous capture and sensing tetracyclines. J Hazard Mater 395:122615. https://doi.org/10.1016/j.jhazmat.2020.122615

Li R, Wang W, El-Sayed EM, Su K, He P, Yuan D (2021) Ratiometric fluorescence detection of tetracycline antibiotic based on a polynuclear lanthanide metal–organic framework. Sens Actuators B 330:129314. https://doi.org/10.1016/j.snb.2020.129314

Li Y, Li J, Zhang Q, Zhang J, Zhang N, Fang Y, Yan J, Ke Q (2022a) The multifunctional BODIPY@Eu-MOF nanosheets as bioimaging platform: a ratiometric fluorescencent sensor for highly efficient detection of F-, H_2O_2 and glucose. Sens Actuators B 354:131140. https://doi.org/10.1016/j.snb.2021.131140

Li Y, Wang Y, Du P, Zhang L, Liu Y, Lu X (2022b) Fabrication of carbon dots@hierarchical mesoporous ZIF-8 for simultaneous ratiometric fluorescence detection and removal of tetracycline antibiotics. Sens Actuators B 358:131526. https://doi.org/10.1016/j.snb.2022.131526

Lima GV, Silva da MR, Fonseca de TS, Lima de LB, Oliveira da de MCF, Lemos de TLG, Zampieri D, Santos dos JCS, Rios NS, Gonçalves LRB, Molinari F, Mattosde MC (2017) Chemoenzymatic synthesis of (S)-Pindolol using lipases. Appl Catal A 546(7):14. https://doi.org/10.1016/j.apcata.2017.08.003

Liu D, Dong C (2020) Recent advances in nano-carrier immobilized enzymes and their applications. Process Biochem 92:464–475. https://doi.org/10.1016/j.procbio.2020.02.005

Liu L, Dai J, Ji Y, Shen B, Zhang X, Linhardt RJ (2021) Detection of protamine and heparin using a promising metal organic frameworks based fluorescent molecular device BZA-BOD@ZIF-90. Sens Actuators B 341:130006. https://doi.org/10.1016/j.snb.2021.130006

Meng F, Ma X, Duan N, Wu S, Xia Y, Wang Z, Xu B (2017) Ultrasensitive SERS aptasensor for the detection of oxytetracycline based on a gold-enhanced nano-assembly. Talanta 165:412–418. https://doi.org/10.1016/j.talanta.2016.12.088

Mo M, Wang X, Ye L, Su Y, Zhong Y, Zhao L, Zhou Y, Peng J (2022) A simple paper-based ratiometric luminescent sensor for tetracyclines using copper nanocluster-europium hybrid nanoprobes. Anal Chim Acta 1190:339257. https://doi.org/10.1016/j.aca.2021.339257

Nunes YL, Menezesde FL, Sousa de IG, Cavalcante ALG, Cavalcante FTT, Moreira da KS, Oliveira de ALB, Mota GF, Souza da JES, Falcão de IRA, Rocha TG, Valério RBR, Fechine PBA, Souza de MCM, Santos dos JCS (2021) Chemical and physical Chitosan modification for designing enzymatic industrial biocatalysts: How to choose the best strategy? Int J Biol Macromol 181:1124–1170. https://doi.org/10.1016/j.ijbiomac.2021.04.004

Pinheiro MP, Rios NS, Fonseca de TS, Bezerra de FA, Rodríguez-Castellón E, Fernandez-Lafuente R, Mattos de MC, Santosdos JCS, Gonçalves LRB (2018) Kinetic resolution of drug intermediates catalyzed by lipase B from Candida antarctica immobilized on immobead-350. Biotechnol Prog 34(4):878–889. https://doi.org/10.1002/btpr.2630

Qian J, Cao N, Zhang J, Hou J, Chen Q, Zhang C, Sun Y, Liu S, He L, Zhang K, Zhou H (2020) Field-portable ratiometric fluorescence imaging of dual-color label-free carbon dots for uranyl ions detection with cellphone-based optical platform. Chin Chem Lett 31(11):2925–2928. https://doi.org/10.1016/j.cclet.2020.05.004

Sanchez A, Cruz J, Rueda N, dos Santos JCS, Torres R, Ortiz C, Villalonga R, Fernandez-Lafuente R (2016) Inactivation of immobilized trypsin under dissimilar conditions produces trypsin molecules with different structures. RSC Adv 6:27329. https://doi.org/10.1039/c6ra03627a

Sheng W, Chang Q, Shi Y, Duan W, Zhang Y, Wang S (2018) Visual and fluorometric lateral flow immunoassay combined with a dual-functional test mode for rapid determination of tetracycline

antibiotics. Microchim Acta 185:404. https://doi.org/10.1007/s00604-018-2945-9
Shi X, Cao B, Liu J, Zhang J, Du Y (2021) Rare-earth-based metal-organic frameworks as multifunctional platforms for catalytic conversion. Small 17:2005371. https://doi.org/10.1002/smll.202005371
Silva ARM, Alexandre JYNH, Souza JES, Neto JGL, de Sousa JPG, Rocha MVP, dos Santos JCS (2022) The chemistry and applications of metal-organic frameworks (MOFs) as Industrial enzyme immobilization systems. Molecules 27(14):4529. https://doi.org/10.3390/molecules27144529
Simon NS (2005) Loosely bound oxytetracycline in riverine sediments from two tributaries of the chesapeake bay. Environ Sci Technol 39:3480–3487. https://doi.org/10.1021/es049039k
Song T, Yu J, Cui Y, Yang Y, Qian G (2016) Encapsulation of dyes in metal–organic frameworks and their tunable nonlinear optical properties. Dalton Trans 45:4218. https://doi.org/10.1039/C5DT03466C
Su P, Zhang A, Yu L, Ge H, Wang N, Huang S, Ai Y, Wang X, Wang S (2022a) Dual-functional UiO-type metal-organic frameworks for the sensitive sensing and effective removal of nitrofurans from water. Sens Actuators B 350:130865. https://doi.org/10.1016/j.snb.2021.130865
Su P, Yu L, Ai Y, Zhang S, Ge H, Bu Y, Huang D, Wang X, Wang S (2022b) Conformational fixation induced fluorescence turn-on of oxytetracycline coordinated on aluminum-based metal-organic frameworks for ultrasensitive sensing application. Sens Actuators B 368:132043. https://doi.org/10.1016/j.snb.2022.132043
Sun T, Hao S, Fan R, Qin M, Chen W, Wang P, Yang Y (2020a) Hydrophobicity-adjustable MOF constructs superhydrophobic MOF-rGO aerogel for efficient oil−water separation. ACS Appl Mater Interfaces 12:56435. https://doi.org/10.1021/acsami.0c16294
Sun C, Dong W, Peng J, Wan X, Sun Z, Li D, Wang S (2020b) Dual-mode fluorescence–SERS sensor for sensitive and selective detection of uranyl ions based on satellite Fe_3O_4–Au@CdTe nanostructure. Sens Actuators B 325:128644. https://doi.org/10.1016/j.snb.2020.128644
Sun P, Yang D, Li J, Zhang Y (2022) Aggregation-induced emission of 4-formyl-3-hydroxybenzoic acid for the ratiometric fluorescence detection of tetracycline antibiotics. Dyes Pigm 197:109841. https://doi.org/10.1016/j.dyepig.2021.109841
Tang Y, Xia T, Song T, Cui Y, Yang Y, Qian G (2018) Efficient energy transfer within dyes encapsulated metal-organic frameworks to achieve high performance white light-emitting diodes. Adv Opt Mater 6:1800968. https://doi.org/10.1002/adom.201800968
Turan E, Sahin F, Suludere Z, Tumturk H (2019) A fluoroimmunodiagnostic nanoplatform for thyroglobulin detection based on fluorescence quenching signal. Sens Actuators B 300:127052. https://doi.org/10.1016/j.snb.2019.127052
Wan Y, Cui Y, Yang Y, Qian G (2021) Nonlinear optical metal-organic frameworks for ratiometric temperature sensing in physiological range. Chin Chem Lett 32(4):1511–1514. https://doi.org/10.1016/j.cclet.2020.10.015
Wang H, Hou F, Jiang C (2005) Ethyl substituted β-cyclodextrin enhanced fluorimetric method for the determination of trace amounts of oxytetracycline in urine, serum, feed of chook and milk. J Lumin 113:94–99. https://doi.org/10.1016/j.jlumin.2004.09.126
Wang Y, Ni P, Jiang S, Lu W, Li Z, Liu H, Lin J, Sun Y, Li Z (2018) Highly sensitive fluorometric determination of oxytetracycline based on carbon dots and Fe_3O_4-MNPs. Sens Actuators B 254:1118–1124. https://doi.org/10.1016/j.snb.2017.07.182
Wang W, Xu Y, Liu X, Peng L, Huang T, Yan Y, Li C (2020) Efficient fabrication of ratiometric fluorescence imprinting sensors based on organic-inorganic composite materials and highly sensitive detection of oxytetracycline in milk. Microchem J 157:105053. https://doi.org/10.1016/j.microc.2020.105053
Wang Y, Li Q, Deng M, Chen K, Wang J (2022a) Self-assembled metal-organic frameworks nanocrystals synthesis and application for plumbagin drug delivery in acute lung injury therapy. Chin Chem Lett 33(1):324–327. https://doi.org/10.1016/j.cclet.2021.06.080
Wang C, Wang C, Zhang X, Ren X, Yu B, Wang P, Zhao Z, Fu H (2022b) A new Eu-MOF for ratiometrically fluorescent detection toward quinolone antibiotics and selective detection toward tetracycline antibiotics. Chin Chem Lett 33(3):1353–1357. https://doi.org/10.1016/j.cclet.2021.08.095
Xing K, Fan R, Du X, Zheng X, Zhou X, Gai S, Wang P, Yang Y (2019) Dye-insertion dynamic breathing MOF as dual-emission platform for antibiotics detection and logic molecular operation. Sens Actuators B 288:307–315. https://doi.org/10.1016/j.snb.2019.03.011
Xing X, Huang L, Zhao S, Xiao J, Lan MS (2020) N-Doped carbon dots for tetracyclines sensing with a fluorometric spectral response. Microchem J 157:105065. https://doi.org/10.1016/j.microc.2020.105065
Xu N, Yuan Y, Yin J, Wang X, Meng L (2017) One-pot hydrothermal synthesis of luminescent silicon-based nanoparticles for highly specific detection of oxytetracycline via ratiometric fluorescent strategy. RSC Adv 7:48429. https://doi.org/10.1039/C7RA09338A
Xu S, Li L, Lin D, Yang L, Wang Z, Jiang C (2022) Rare-earth ions coordination enhanced ratiometric fluorescent sensing platform for quantitative visual analysis of antibiotic residues in real samples. Chin Chem Lett. https://doi.org/10.1016/j.cclet.2022.107997
Yang K, Jia P, Hou J, Bu T, Sun X, Liu Y, Wang L (2021) Innovative dual-emitting ratiometric fluorescence sensor for tetracyclines detection based on boron nitride quantum dots and europium ions. ACS Sustain Chem Eng 8:17185–17193. https://doi.org/10.1021/acssuschemeng.0c05872
Yoo J, Ryu U, Kwon W, Choib KM (2019) A multi-dye containing MOF for the ratiometric detection and simultaneous removal of $Cr_2O_7^{2-}$ in the presence of interfering ions. Sens Actuators B 283:426–433. https://doi.org/10.1016/j.snb.2018.12.031
Yuan M, Jin Y, Yu L, Bu Y, Sun M, Yuan C, Wang S (2023) Europium-modified carbon nitride nanosheets for smartphone-based fluorescence sensitive recognition of anthrax biomarker dipicolinic acid. Food Chem 398:133884. https://doi.org/10.1016/j.foodchem.2022.133884
Zahirinejad S, Hemmati R, Homaei A, Dinari A, Hosseinkhani S, Mohammadi S, Vianello F (2021) Nano-organic supports for enzyme immobilization: scopes and perspectives. Colloids Surf B 204:111774. https://doi.org/10.1016/j.colsurfb.2021.111774
Zhang Y, Gutierrez M, Chaudhari AK, Tan J (2020) Dye-encapsulated zeolitic imidazolate framework (ZIF-71) for fluorochromic sensing of pressure, temperature, and volatile solvents. ACS Appl Mater Interfaces 12:37477–37488. https://doi.org/10.1021/acsami.0c10257
Zhang J, Bao Z, Qian J, Zhou H, Zhang K (2022) Copper doped zinc sulfide quantum dots as ratiometric fluorescent probes for rapid and specific detection of tetracycline residues in milk. Anal Chim Acta 1216(11):339991. https://doi.org/10.1016/j.aca.2022.339991
Zhao Y, Liu J, Han M, Yang G, Ma L, Wang Y (2021) Two comparable Ba-MOFs with similar linkers for enhanced CO_2 capture and separation by introducing N-rich groups. Rare Met 40:499–504. https://doi.org/10.1007/s12598-020-01597-w
Zhu Q, Xu Q (2014) Metal–organic framework composites. Chem Soc Rev 43:5468. https://doi.org/10.1039/C3CS60472A